Global Navigation Satellite Sounding of the Atmosphere and GNSS Altimetry: Prospects for Geosciences

T. P. Yunck and G. A. Hajj

Jet Propulsion Laboratory, California Institute of Technology, Pasadena, California

The vast illuminating power of the Global Positioning System (GPS), which transformed space geodesy in the 1990s, is now serving to probe the earth's fluid envelope in unique ways. Three distinct techniques have emerged: ground-based sensing of the integrated atmospheric moisture; space-based profiling of atmospheric refractivity, pressure, temperature, moisture, and other properties by active limb sounding; and surface (ocean and ice) altimetry and scatterometry with reflected signals detected from space. Ground-based GPS moisture sensing is already in provisional use for numerical weather prediction. Limb sounding, while less mature, offers a bevy of attractions, including high accuracy, stability, and vertical resolution; all-weather operation; and exceptionally low cost. GPS bistatic radar, or "reflectometry," is the least advanced but shows promise for a number of niche applications.

INTRODUCTION

Atmospheric sounding with the Global Positioning System arose in the 1980s from GPS geodesy. It had long been expected that signal delays through the neutral atmosphere would ultimately limit the accuracy of all forms of space geodesy [*Abshire and Gardner*, 1985; *Davis et al.*, 1985]. The major concern was the variable effects of water vapor, which represented the greatest model uncertainty. Early investigators explored a variety of techniques for reducing that critical error. A particularly effective strategy involved modeling the atmospheric delay as a random walk and estimating a delay correction directly from the GPS data at every time step – typically every few minutes [*Lichten and Border*,1987; *Lichten and Bertiger*, 1989].

Although atmospheric delay estimates were at first treated as "nuisance" parameters, analysts soon found that by using surface pressure data to calibrate the delay due to dry air they could recover the delay due to moisture with exceptional fidelity [*Elgered et al.*, 2003]. This "wet" delay can be readily converted to an estimate of precipitable water (PW) for use in weather and climate modeling. Alternatively, one can assimilate the delay estimates themselves directly into numerical models [*Ha et al.*, 2003; *Ridal and Gustafsson*, 2003]. The GPS geodetic ground networks now expanding rapidly around the world are thus yielding a windfall of atmospheric moisture data, one of the most critical quantities for numerical weather prediction (NWP).

Over the past decade, a number of weather organizations have been investigating ground-based GPS sounding (see, for example, the papers from the first International Workshop on GPS Meteorology in Tsukuba, Japan, Jan 2003,

and the Second CHAMP Science Meeting in Potsdam, Sep 2003). Plate 1 shows a sequence of PW contour maps derived from GPS data by the Japanese Meteorological Agency [*Hatanaka*, 2003] at the sites of Japan's vast GEONET array. The maps span a 3-day period in September 2001, as a weather system moved across the islands.

GROUND-BASED GPS AND WEATHER PREDICTION

The keen interest in GPS PW data stems from its potential for improving weather prediction, from short-term "now-casting" out to 10 days and beyond. For several years the Forecast Systems Laboratory (FSL) of the US National Oceanic and Atmospheric Administration (NOAA) has produced daily experimental predictions across the continental US of such quantities as relative humidity (RH) and precipitation, with and without GPS PW assimilated along with other standard data sources [*Gutman et al.*, 2003]. Plate 2 summarizes the 12-hr RH predictions from 2000 through 2002, with statistics collected into 1-month bins. The scale on the left gives the average effect of the GPS data, in percent accuracy change, for the full month. Values are given for four different altitudes (or, more precisely, pressure levels) for each month.

The GPS data have a consistently beneficial effect, except at the highest altitude, where ground-based GPS offers no useful discrimination. While the overall impact may appear small, these improvements are significant given the large volume of other data already assimilated. Furthermore, the average values are deceptive. Most days are relatively benign, without marked weather activity. The challenge for weather prediction is not the majority of easy days when forecasts are reliable, but those rarer days where major transitions and serious weather events are in progress or pending, and which are often inaccurately forecast. The value of the GPS data on those days tends to be higher than is suggested by the monthly averages.

A limitation of these early assimilation efforts is their restriction to a scalar PW value at each time step, representing the integrated zenith moisture for each observing site. This value is then related to other elevations by means of a mapping function, a method that is only approximate and that necessarily misses direction-dependent irregularities. Such irregularities can be pronounced at moist sites, particularly at times when weather systems are active. Because the mapping function does not fit these irregularities, they will show up in the post-fit residuals, combined with such other errors as instrumental noise, signal multipath, and higher order ionospheric effects. It is reasonable to presume that in many conditions the moisture irregularities will dominate the post-fit residuals and, therefore, that by adding back the residual to the mapped zenith delay solution one might obtain a value closer to the true line-of-sight moisture between the receiver and transmitter. That is the

Plate 1

Plate 2

approach now being taken by several research groups seeking to improve ground-based GPS meteorology [*Braun and Rocken*, 2003; *Shoji et al.*, 2003].

There remain, however, important limitations to ground-based GPS sounding: It yields just one principal product, integrated PW; it offers little useful vertical resolution; and it is restricted to land areas fitted with extensive GPS networks. It is not, in short, a global solution. Space-based atmospheric limb sounding offers a valuable complement that addresses all of these issues.

ATMOSPHERIC SOUNDING FROM SPACE

In the late 1980s a few groups began to consider the possibility of atmospheric limb sounding from Earth orbit by radio occultation, exploiting GNSS signals as sources. This was inspired by the great success of planetary radio occultation over the previous 25 years, beginning with the 1964 Mariner IV mission to Mars [*Fjeldbo*, 1964; *Kliore et al.*, 1964]. Although Earth radio occultation had been proposed in various forms since the 1960s, the first account of a practical approach exploiting GPS did not appear until *Yunck et al.* [1988]. Progress has since been rapid. The first successful space-based demonstration of GPS occultation was the 1994 GPS/MET experiment, led by the University Corporation for Atmospheric Research (UCAR) in Boulder [*Rocken et al.*, 1997]. For a more complete history of radio occultation see *Melbourne et al.* [1994] and *Yunck et al.* [2000].

Plate 3 illustrates the GNSS occultation geometry. A low Earth orbiter (LEO) at a typical altitude of 400-800 km, equipped with limb-directed antennas, tracks GNSS signals as they rise and set through the atmosphere. The receiver continuously measures the changing carrier phase at both L-band frequencies. The atmosphere acts as a lens, bending and retarding the signals, inducing an excess path delay. This delay appears in the measurements as additional accumulated phase and a Doppler shift. Depending on the observing geometry, it may take a minute or more for the observed signal to pass from the top of the neutral atmosphere (~100 km altitude) to the surface, or vice versa. Since the changing geometry is dominated by the rapid orbital motion of the LEO, most soundings occur within ±45° of the forward and reverse velocity directions.

Plate 4 shows the geographical distribution of soundings over 24 hours from a single high-inclination receiver for a 24-satellite GPS constellation. There are roughly 700 in all. With a future GNSS constellation of 60 satellites, a 12-element LEO occultation array will darken the coverage map, acquiring more than 15,000 soundings daily. Both Galileo and the "Block 3" GPS satellites, to be deployed within the next decade, will boost signal strength by 6 dB above today's levels, improving both retrieval quality and consistency of penetration to the surface.

Plate 3

Plate 4

Sounding the atmosphere by radio occultation differs fundamentally from ground-based geodetic delay estimation. Because we are looking at (usually) a single ray traversing the atmosphere horizontally, we obtain extremely high vertical resolution – of the order of 100 m from the surface to the stratosphere. Moreover, radio occultation delivers a diverse assortment of atmospheric parameters distributed almost uniformly around the globe, enabling a broader variety of weather and climate applications [*Anthes et al.*, 2000]. In addition, from the precisely known observing geometry we can compute the absolute height of each measurement with respect to the geoid (or other reference surface) to within a few meters, limited largely by horizontal structure. This allows construction of precise 2D contour maps, pressure gradients, and such derived products as geostrophic wind fields in the troposphere and stratosphere [*Leroy*, 1997]. This ability to extract precise "geopotential heights" is unique among spaceborne sensors. The basic retrieval method, yielding initial profiles of atmospheric refractivity, density, pressure, and temperature (or moisture), is summarized below.

Profile Retrieval

To begin, we must first isolate the atmospheric excess delay from the measured total phase by precise geometric modeling and dual-frequency ionospheric correction, and then compute the atmosphere-induced Doppler shift. From this one can derive a precise estimate of the changing bending angle along the full vertical profile. The bending angle depends directly on the atmospheric refractivity, which one can compute by means of an Abel integral inversion. (For these steps we assume local spherical symmetry in the atmosphere, a usually adequate approximation). The water molecule's permanent dipole moment causes moisture to affect atmospheric refractivity more strongly than dry air. In the dryer regions, above about 5 km altitude, we can ignore the effect of moisture on signal refraction. The refractivity then depends only on the number density of atmospheric molecules and their types. Since we know the molecular weights of the different species and their relative abundance we can compute the atmospheric density accurately along the profile. And since the pressure field is in near hydrostatic equilibrium, we can sum up the total weight of a column of air from the top downwards to determine atmospheric pressure along the profile. With pressure and density known, we can apply the standard gas laws to derive the temperature profile.

Moisture in the lower troposphere can increase the path delay markedly, particularly in the tropics, where it can contribute up to 30% of the refractivity. Because of the little variability of temperature in that region, one can apply climatology (or other external information) to extrapolate the temperature profile downward and estimate moisture.

(For a more thorough discussion see *Hajj et al.* [2002].) The processing sequence thus proceeds as follows:

- Isolate the atmospheric excess phase and compute the observed Doppler shift.
- Compute a profile of the signal bending angle from the changing Doppler shift.
- Compute a refractivity profile from the bending angle by an Abel integral inversion.
- Compute a molecular density profile from the observed refractivity and known atmospheric constituents.
- Compute a pressure profile from molecular density and known molecular weights, summing from top down.
- Compute a temperature profile from standard gas laws, or…
- In the lower troposphere, model the temperature and estimate moisture density.

There are several sophisticated variations on this approach, most notably the one-dimensional variational (1DVAR) method, which derives temperature and humidity jointly by use of atmospheric models with assigned a priori values and variances, along with the measured refractivity [*Kursinski et al.*, 2000; *Palmer et al.*, 2000]. Complications often arise in deriving signal bending in the lower troposphere as a result of atmospheric multipathing and signal loss from super-refraction, or "ducting." At present only about 70% of retrievals reach the lowest 1 km. "Open-loop" signal acquisition and advanced retrieval techniques will soon largely remove the multipath issue, while other specialized algorithms now under study promise to improve recovery below ducting layers [*Gorbunov et al.*, 1996; *Gorbunov*, 2001 & 2002; *Ao et al.*, 2003; *Sokolovskiy*, 2003]. A new generation of sensors and retrieval algorithms, to debut operationally on COSMIC in 2005 or 2006 [*Lee et al.*, 2000], should reach the lowest 1 km in more than 90% of profiles globally.

Performance

It may be surprising that this sequence of steps with its various approximations can yield useful accuracy. The key is in the precision with which we can measure the GPS carrier phase. A geodetic receiver with an antenna gain of 6-10 dB can measure the instantaneous phase with a precision of a few millimeters in a fraction of a second. With the power of modern GNSS-based orbit determination we can recover the atmospheric Doppler shift observed from low orbit to about 0.1 mm/s. At 70 or 80 km altitude the atmospheric path delay is negligible, even at the level of millimeters. That delay grows exponentially as the ray descends, reaching up to 2.5 km at the surface within about 60 s, with phase rates exceeding 100 m/s, or nearly a million times the precision of the measurement. The standard

analysis assumptions – local spherical symmetry, hydrostatic equilibrium, mixing ratios of atmospheric constituents – while imperfect, are extremely good in most conditions and result in relatively small errors.

In the first performance analysis for GPS limb sounding, conducted in March 1988, the JPL team estimated that temperature accuracies of a few tenths of a Kelvin might be achieved over altitudes ranging from about 5 to 30 km [*Yunck et al.*, 1988]. More detailed studies in later years [*Kursinski et al.*, 1997; *Hajj et al.*, 2003] supported this conclusion. These studies suggest that because the major errors tend to be random or quasi-random, averaging of multiple profiles for long-term climate studies could reduce the effective temperature error below 0.1 K. That is, the averaged profiles may be accurate, independent of the instrument used, to better than 0.1 K over an extended altitude range. This would represent an improvement by a factor of anywhere from 10 to 40 over current global techniques, depending on just where the occultation error bottoms out (0.05 K?) and what one believes to be the long term stability of other techniques (of order 1-2K).

Climate Signal Detection

Arguably, the greatest concern in Earth science today is global climate change. That is the focus of NASA's Earth science program, exemplified by the flagship spacecraft of the Earth Observing System – Terra, Aqua, and Aura – and the dozen or so specialized probes, such as GRACE and ICESat, now in operation. Many more international missions, in flight or in preparation, address related themes.

A central question is whether or not Earth has entered a period of accelerated global warming (as seems likely) and, if so, to what extent this may result from stresses imposed by human activity. While the evidence from both ground and space is compelling [*Mann et al.*, 2003; *Vinnikov and Grody*, 2003; *Cubasch et al.*, 2001], to discern the effects of distinct drivers and trace the operative climate processes we require accurate data at all levels of the atmosphere. Despite vast investments in sensors we are at present severely limited in our ability to gather such data globally.

The United Nations Intergovernmental Panel on Climate Change (IPCC) has estimated that human-induced global warming may be in the range of 0.1-0.3 K per decade at the surface over the next 20 years, and 0.2-0.5 K per decade over the next century. The effects may be subtler (or even reversed) in upper strata. Plate 5 shows global temperature projections for a variety of climate models [*Cubasch et al.*, 2001]. Detecting such signals requires great measurement precision and long-term stability: 0.1 K/decade or better. Current spaceborne instruments fall well short of this. The sensor suite is dominated by passive infrared and microwave radiometers, including MISR, MODIS, MLS,

Plate 5

6

AIRS/AMSU, and AVIRIS. Although great ingenuity is employed to maintain calibration, over a decade or more this is elusive. Sensor aging and replacement with new designs undermine stability. Even external calibration against in situ radiosondes is limited by the variable quality of the radiosonde record. Over a decade or more the best that can reasonably be achieved is 1-2 K absolute stability. Thus, current sensors lack by at least an order of magnitude the stability needed to address some of the most critical questions facing Earth science.

In a 2002 research solicitation NASA declared: "Perhaps the greatest roadblock to our understanding of climate variability and change is the lack of robust and unbiased long-term global observations." They went on to say that for climate monitoring "the focus is on…construction of consistent datasets from multi-instrument [and] multi-year observations with careful attention to calibration and validation over the lifetime of the measurement" [*NASA*, 2002].

GNSS occultation exploits principles entirely different from those of radiometers, depending primarily on the timing of delay variations over about one minute – something we can accomplish with extreme accuracy. Each profile is largely self-calibrating and virtually unbiased, independent of the particular instrument used or when in its lifetime the profile is acquired. Individual and averaged profiles will therefore maintain their accuracies through future instrument evolution, indefinitely. A profile taken today will be directly comparable, at the level of 0.1 K or better, with a profile taken 50 years hence, no matter the specific designs of the instruments or the frequencies and structures of the signals employed.

The consequences for research in climate change could be profound. For the first time we will have the means to detect atmospheric temperature trends (above ~5 km) at the level of 0.1 K within a matter of years. Moreover, GNSS occultation can provide a continuing source of calibration data to normalize and stabilize atmospheric products from sensors now in place, transforming them into effective climate sensors. In short, if its current promise is validated, GNSS radio occultation may offer a key to removing the "greatest roadblock to our understanding of climate variability and change."

Early Experimental Results

Establishing average temperature accuracies of 0.1 K or better over a broad altitude range presents difficulties. The challenge is to find adequate standards of comparison. To date, the primary standards have included radiosonde data and climate analyses generated by the US National Centers for Environmental Predictions (NCEP) and by the European Centre for Medium-Range Weather Forecasts (ECMWF), derived by assimilating radiosonde and space

data into numerical models. For the former we must find radiosondes that are close in space and time to the profiles to be validated. While we can map the analyses to any time and location, they involve a good deal of interpolation and spatial smoothing. In neither case can we expect better than 1-2 K accuracy from the comparison data.

Plate 6 shows a temperature profile produced at JPL in 1995 from GPS/MET data, compared against both a radiosonde and the ECMWF analysis. Agreement is consistent with the expected 1-2 K accuracy of the analysis. The lack of fine vertical detail in the analysis suggests that its inherent smoothing has compromised vertical resolution. From such tests we cannot assess the accuracy of the GPS data beyond the evident level of agreement. Figure 1 shows the average agreement with ECMWF climate analyses for several hundred GPS/MET profiles. The standard deviation (shaded area) over an altitude range of 5-25 km is roughly 2 K. The mean difference (solid line) over the same range is reduced to 0.5-1.0 K, well off the 0.1 K or better predicted for the GPS occultations alone.

A new generation of occultation receiver, JPL's Black-Jack, first flew on the German CHAMP mission in July of 2000. Plate 7 shows a statistical summary of more than 4000 CHAMP refractivity profiles from May and June 2001, compared with ECMWF daily analyses [*Beyerle et al.*, 2003]. The GFZ analysis team applied two different techniques, the standard "geometric optics" technique described above (blue), and a "canonical transform" technique (red) [*Gorbunov*, 2002], which offers the advantage of separating multiple tones in the lower troposphere and enhancing vertical resolution. The solid curves are for the whole earth, while the dashed curves are for the northern hemisphere, for which, owing to more abundant radiosonde data, the analyses are more reliable. Mean offsets (right) and standard deviations (left) correspond roughly to temperature mean offsets of 0.5 K and sigmas of 1-2 K, above 2-3 km. That level of temperature agreement is shown explicitly in *Hajj et al.* [2003]. These values do not differ appreciably from the earlier GPS/MET results and leave open the question of actual GPS occultation accuracy.

CHAMP / SAC-C Comparisons

Analysis prospects improved markedly when the Argentine SAC-C spacecraft, carrying a second BlackJack receiver, reached orbit in November of 2000. For the first time we could compare data directly from two advanced occultation instruments, provided they observed the same location at about the same time. It happens that such coincidences are rare but not unknown. Of more than 60,000 soundings acquired from 10 July 2001 to 9 June 2002, sixty pairs occurred within 200 km and 30 min of one another. Of those, fewer than thirty pairs occurred within 100 km

Plate 6

Fig 1

Plate 7

8

and 30 min. As these coincidences are not exact there are real differences between pairs, estimated to be typically several tenths of a Kelvin.

Plate 8 compares near-coincident CHAMP and SAC-C occultations. The left panel shows a typical coincident pair (solid red and green) plotted against standard NCEP and ECMWF analyses computed for the two profiles. The observing directions differed by 137°. What stands out is the closeness of the two occultation profiles despite their differences in space and time. Both differ from the analyses, which are similar to one another but again lack fine vertical detail. This provides stronger evidence of the essential correctness of the occultation result. The NCEP and ECMWF analyses involve a fair degree of smoothing and cannot reliably capture such sharp features as the tropopause at ~9.5 km shown in the occultations. That two profiles acquired from different instruments and directions agree so exactly in this detail is compelling.

Plate 8 also shows the mean differences and sigmas for all occultation pairs coincident within 30 min, for maximum separations ranging from 100 to 300 km. Between 5 and 25 km altitude the average differences fall within or near 0.1 K. Compare this with Fig. 1 showing differences with the weather analyses, where the mean offsets are about 5 times greater. For the closest pairs, the sigmas (when reduced by root-2 to account for the combining of two profiles) are near 0.5 K at 20 km and below. These increase steadily for the more widely separated pairs, at least partly because of actual differences between the locations. For a more thorough presentation see *Hajj et al.* [2003].

While these results are consistent with an occultation bias of 0.1 K or less, they do not prove it. There could be, for example, common biases or trends in the occultation profiles not revealed in these comparisons. We know that at higher altitudes where the retrieval is initialized (above 30 km), and near the surface where the observations can become corrupted by complex atmospheric effects, biases can creep in. Their causes, however, are well understood [*Sokolovskiy*, 2001a; *Beyerle et al.*, 2003a; *Ao et al.*, 2003; *Sokolovskiy*, 2003]. Refined techniques now in development may all but eliminate refractivity biases near the surface and extend the upper range of profile accuracy.

Retrieving Moisture Profiles

GNSS occultation is often faulted for its inability to distinguish the refractive effects of moisture and dry air, leading to uncertainties in the structures and behaviors of the lower troposphere. While this is true in the strictest sense – the pure measurement does not allow a deterministic separation – as with nearly all science data there is a rich and informative context: physical constraints, spatial and tem-

Plate 8

9

poral signatures, external and meta data to supply further clues. Sharp gradients, for example, cannot be sustained in dry air. In moist regions refraction from water begins to dominate below 5 km altitude. A simple tactic is to use temperature from a weather analysis to estimate moisture near the surface from the refractivity signature. *Kursinski and Hajj* [2001] show that this can yield moisture with a precision of 0.2 g/kg, surpassing other remote sensing instruments. More promising is the direct assimilation of bending angles or refractivity profiles into numerical models for a more nuanced separation of effects. Some scientists have begun to examine the additional information in glancing surface reflections (discussed below) and in polarization effects. As these cues become better understood and the models correspondingly refined, such approaches are likely to provide further gains.

Table 1. Seven Attractions of GNSS Occultation

- Offers order-of-magnitude improvement in accuracy and long-term stability of atmospheric temperature profiles.
- Operates undiminished in all weather, day or night.
- Offers near-uniform global coverage from the upper stratosphere to the surface.
- Provides vertical resolution to better than 100 m throughout the troposphere.
- Yields absolute heights of measured quantities to better than 10 m, permitting derivation of global pressure contours and non-equatorial geostrophic wind fields.
- Exploits different physical principles from other atmospheric sensors, remote or in situ, presenting an independent comparison and calibration standard.
- Requires only a palm-sized module costing <1 % of the tens to hundreds of M$ of many of today's passive sensors.

Early Assimilation Studies

Perhaps the greatest appeal of GNSS occultation is its potential for improving weather forecasts. As yet, with the still meager supply of high quality occultation data, little has been accomplished in the way of data assimilation and impact studies. But what has been done shows much promise. Preliminary assimilation studies have been reported by *Zou et al.* [2003], *Healy et al.* [2003], *Kuo et al.* [2003], and *Aoyama et al.* [2003]. In the first of these, Zou et al. assimilated CHAMP bending angle data taken over a two-week period in July 2002. This approach is attractive because the effect of refractivity along the ray path can be modeled, ionospheric effects are more readily removed, and problems unique to refractivity retrieval (e.g., the upper boundary condition, various limiting assumptions, and the ill-posed nature of the inversion under super-refraction) can be avoided. By contrast, the Healy and Kuo teams chose the more tractable refractivity profiles for assimilation, and Aoyama et al. assimilated the final temperature profiles.

Despite the extreme sparseness of the data sets, all reported slight improvements in forecasts of various kinds – some going out 4 or 5 days – when occultation data were included. Healy et al. note that the "results are very encouraging [and] support the case for assimilating RO measurements operationally."

Despite these successes GNSS occultation science is still in its infancy. The gulf between the tens of profiles used in assimilations today and a future of tens of thousands is beyond our power to bridge by intuition. Table 1 tabulates seven key attractions – the Seven Cardinal Virtues – of GNSS limb sounding. Soon this simple trick of radio metrology may offer a key to one of the most vexing problems in Earth science: discerning the faint signatures of global climate change. The potential for monitoring of the global troposphere has equally profound implications for weather prediction.

GNSS SURFACE REFLECTIONS

Traditional radar altimetry (e.g., TOPEX/Poseidon and Jason-1) observes vertically, obtaining one nadir height value at a time. GNSS reflectometry, by contrast, can track a dozen or more surface returns from many angles at once with a single LEO receiver. This offers the prospect of higher temporal and spatial resolution for resolving finer scale, short-lived features, such as mesoscale eddies [*Treuhaft et al.*, 2003], which play an important role in the transport of momentum, heat, salt, nutrients, and chemicals within the ocean. Mesoscale eddies are analogous to atmospheric storms and create mean sea-height changes of about 10 cm over distances of 10-100 km, persisting typically for 1 week to 1 month. Ocean coverage from a single orbiting receiver collecting reflections from 24 GPS satellites is illustrated in Fig. 2. *Hajj and Zuffada* [2003] show that an array of eight orbiters acquiring GPS and Galileo reflections could provide global 3-cm ocean heights in one day with 200-km spatial resolution, or sub-decimeter heights in four days with 25-50 km resolution.

Another attractive application is the monitoring of barotropic waves that move across ocean basins too quickly to be captured within the Jason-1 10-day repeat cycle [*Stammer et al.*, 2000]. While the technical feasibility of bistatic GNSS is clear, it remains to be seen whether it will offer practical advantages over alternative approaches, such as wide swath altimetry [*Rodriguez and Pollard*, 2001] or flying multiple nadir altimeters [*Raney*, 2001a,b; *AVISO*, 2003]. Here we consider some basic requirements and configurations for a practical bistatic GNSS system.

An early concept for GNSS-based ocean altimetry was proposed by *Martin-Neira* [1993]. Since then a good deal of theoretical system performance analysis has appeared [*Picardi et al.*, 1998; *Zavorotny and Voronovich*, 2000; *Fung et al.*, 2001; *Hajj and Zuffada*, 2003]. The first

Fig 2

11

known GPS ocean reflection observed from space was collected fortuitously by the SIR-C L-band radar carried aboard the space shuttle (STS-68) in 1995, and detected in an intensive search by a team at JPL several years later [*Lowe et al.*, 2002].

A Few Principles of GNSS Reflectometry

The ocean reflects incident signals to an orbiting receiver from an extended portion of the surface. A given transmitted wavefront will arrive first from the specular reflection point, representing the shortest reflection path. Steadily decreasing energy is received from surrounding points, incurring greater path delays. By cross-correlating the received signal against a model signal at many different closely spaced delays one can map the returned energy vs delay. Figure 3 shows the nominal shape of the cross-correlation function for the direct GPS signal, assuming no multipath (left), along with typical cross-correlation functions for a signal reflected from the rough ocean surface, for different surface wind speeds. Because the greatest reflected energy arrives on the shortest path, the function rises abruptly, then decays gradually as the weaker outlying reflections trail in. The detailed shape of this function contains a good deal of information about the ocean surface. To extract this information, the receiver must provide hundreds of individual correlators to map the correlation functions from a dozen or more concurrent reflections.

The sharp leading edge of the correlation function permits precise determination of the arrival time – and hence total delay – of the reflection from the specular point; from that delay, along with other geometrical modeling information, one can derive an estimate of the ocean height at that point. Analysis of the correlation tail can reveal information about the surface roughness, significant wave height, and wind speed. Thus, from the same reflections one can, in principle, perform both altimetry and scatterometry.

Practical Considerations

Many technical challenges arise in making such measurements from Earth orbit (for a succinct discussion see *Hajj and Zuffada*, 2003). Among these are the weakness of the reflected signals, the wide angular extent over which reflections may be seen (ranging from nadir to the Earth horizon) and the rapid signal de-coherence due to ocean roughness, which is typically large in comparison to the ~20 cm GNSS wavelengths. The last of these implies that under most ocean surface conditions and viewing geometries we cannot acquire the continuous phase observable that is so essential in many precise GNSS applications. Instead we must rely on heavily averaged pseudorange measurements to recover signal delay and ocean height. That task is made more difficult by the weak signal, neces-

Fig 3

sitating antenna gains of 20 dBIC or greater. High gains imply large collecting areas, in this case at least 2 m^2. Moreover, to attain the precision and spatial resolution needed to study ocean eddies, we must seek to acquire nearly all detectable reflections, of which (with GPS and Galileo) there may be a dozen or more at once. Thus, we require a bouquet of beams that can be steered broadly and independently. This is further complicated by the varying polarizations of signals reflected from different angles. A good deal of creative design is needed to devise efficient systems that can compete with more traditional techniques.

There are, however, reasons for optimism. Among the less obvious properties of bistatic GNSS is the complex dependence of observation quality on viewing angle. For a given delay measurement precision, the greatest sensitivity to ocean height occurs at nadir. This sensitivity degrades roughly as 1/cos of the angle off nadir. However, reflected signal quality is poorest at nadir, owing both to a lower returned signal strength and greater decoherence. The delay accuracy can improve by a factor of two or more at 60° off nadir. Figure 4, from *Hajj and Zuffada* [2003], shows the expected L1 reflected range measurement error as a function of the angle off nadir for different antenna gains. In addition, for a given observation beamwidth the number of reflections to be seen is least at nadir. As the beam moves off nadir it subtends increasingly large surface areas, and those areas exhibit greater curvature (hence more angles that reflect to the sensor). Figure 5 quantifies this tradeoff for a receiver at 700 km. At the horizon the average number of reflected signals within a unit solid angle is fully two orders of magnitude greater than at nadir.

Fig 4

Fig 5

OCCULTATION / REFLECTION SYNERGY

New realms of investigation often bring surprises and GNSS reflectometry is no exception. We've noted that the coherence time of the reflected signal tends to increase with increasing angle off nadir. The Rayleigh criterion is traditionally used to define the onset of incoherent scattering and is given by

$$h = \lambda / 8\sin \varepsilon,$$

where h is the wave height, λ is the signal wavelength, and ε is the observing angle with respect to a tangent line at the reflection point. This says simply that when ocean wave heights exceed h, delays from the crest and trough differ by more than $\lambda/4$, leading to loss of coherence. In Fig. 6 we plot h as a function of the angle off nadir for a LEO at 700 km. For normal incidence (nadir reflection) the ocean scatters coherently only for h <2 cm; near the horizon (~64° off nadir) this occurs for h <1 m. The former condition is almost never satisfied while the latter is satisfied much of the time.

Fig 6

GNSS satellites broadcast their signals with right-hand circular polarization (RCP). For a reflection directly at nadir this is fully reversed, requiring an LCP antenna. For reflections off nadir the polarization reversal is only partial; hence they contain both RCP and LCP components. Glancing reflections near the horizon remain predominantly RCP and thus can be detected with a standard RCP GNSS antenna. We see then that reflections visible well off nadir offer a suite of attractions: they are typically stronger, having reflected from a considerably larger surface area; they have longer coherence times, approaching continuous coherence (and thus offering the power of the centimeter-quality phase observable) near the horizon; and they can be acquired with a standard RCP antenna. Evidently, we have not yet exhausted the virtues of GNSS limb sounding. To the seven listed earlier we can add the prospect of acquiring high-precision glancing surface reflections. Figure 7 illustrates the geometries for nadir and near-limb reflections.

Recent Observations

This indeed is more than just a prospect. Plate 9 shows a spectrogram of a typical GPS occultation acquired by CHAMP. The horizontal axis is frequency and the vertical axis is time (advancing downward), which can also be thought of as altitude, decreasing with time as the occultation descends. The changing frequency of the occulting signal, including the gross effect of the atmosphere, has been removed, so we see the occultation as the bright, nearly constant-frequency vertical feature. Small frequency variations, including occasional splitting of the signal into two or more tones in the lower troposphere, result from atmospheric structure and provide the basic information of the measurement. Also evident in Plate 9 is a more curious feature: a faint line slanting in from the left edge, intersecting the occultation near the surface. A similar feature appears in a high percentage of CHAMP and SAC-C occultations. While these were at first puzzling, analysts at JPL and GFZ quickly discerned them to be glancing reflections of the occulting signal – essentially a form of multipath.

Students of GPS will know that because of the pseudonoise (PN) code modulation on the GPS signals, when the receiver tracks a direct signal, any reflection that is delayed by more than 1.5 code chips (about 45 m for the P-code and 450 m for the C/A-code) with respect to the direct signal is largely suppressed. Only when the occultation is relatively near the surface and the excess reflected delay is sufficiently small can we expect to see the glancing reflection, and then it will be attenuated owing to its offset from the modeled code. Future upgrades to the receiver software will anticipate these reflections and model them directly in order to recover them at full strength.

Fig 7

Plate 9

The CHAMP science team at GeoforschungZentrum (GFZ) in Potsdam has done a thorough study of these glancing reflections, with promising results [*Beyerle et al*, 2002]. Figure 8 shows all occultations acquired by CHAMP over a 4-week period in the spring of 2001 (dots) together with all detected reflections (circles). Clearly evident is the relative scarcity of reflections in the tropics. This is presumed to owe to the combination of dense tropical moisture, attenuation from the PN code offset, and the less frequent penetration of tropical occultations sufficiently close to the surface to yield the required small delay offsets. With coming refinements in "open-loop" signal acquisition [*Sokolovskiy*, 2001b, 2002] and direct onboard modeling of the reflections, this shortfall should be considerably alleviated.

Also evident in Fig. 8 is the presence at high latitudes of reflections in almost equal densities from water and ice, offering the possibility of cryosphere as well as ocean sensing. In fact, at high latitudes nearly all occultations occurring over water or ice are accompanied by a detectable reflection. These uninvited guest signals may effectively double the science value of occultation sensors, a reward we can realize with relatively simple flight software updates. We are thus seeing an unexpected convergence of GNSS occultation science and reflectometry.

In their scrupulous analysis, Beyerle et al. chose as their fundamental observable the anomalous Doppler shift (evident in Plate 9) of the reflected signal. They show that this depends on a number of factors, including the height of the reflecting surface, its slope (when ice), and the moisture density of the atmosphere. They argue that in different circumstances the Doppler signal may be used to estimate each of these. For example, for ocean reflections, where the height and slope are known, one can estimate moisture in the lower troposphere. In frigid regions, where atmospheric moisture is negligible, one can recover topography to investigate ice mass balance and the evolution of ice sheets – central issues in global climate change. More recently, *Cardellah et al.* [2003] showed how one can analyze the direct and reflected signals interferometrically to infer ice height with possible sub-decimeter accuracy.

THE BLACKJACK OCCULTATION RECEIVER

Plate 10 shows the 48-channel BlackJack receiver now flying on CHAMP and SAC-C. That model is based on c. 1997 technology and by no means exploits the level of integration possible even then. Also shown is a postage-stamp-size 12-channel consumer GPS receiver of the kind now found in cell phones and wristwatches. While far less capable than the BlackJack, it illustrates what we have

Fig 8

Plate 10

come to expect in consumer electronics and hints at a possible future for GNSS flight sensors. We note that consumer electronics – laptop computers, PDAs, DVD players – are now flown routinely on the space shuttle and space station in just the sorts of low orbits favored for occultation and reflection sensing.

To achieve its high performance, the BlackJack itself is made almost entirely of commercial (rather than flight rated) electronic parts. The BlackJack and its predecessor, the TurboRogue Space Receiver, have now accumulated well over 60 years in space without an on-orbit failure. The occasional radiation-induced single-event upset (typically one every week or two on SAC-C) is cleared within minutes by an automatic software reset. Plate 11 shows a concept for a more highly integrated GNSS science receiver based on current digital technology, an area that continues to advance swiftly. Such a device could be reproduced even in limited quantities (ignoring development costs) for less than $50,000 apiece.

In the context of commercial electronics, $50,000 for the module in Plate 11 may seem high. In the world of space-borne sensors, however, that is a trifle. Typical acquisition costs for sensors like MODIS, MISR, AIRS/AMSU, ATMS, and so on, are many tens of millions of dollars. Once built, such a module could be carried by a great variety of LEO spacecraft. What is more, most satellites today carry GPS for navigation and timing. Reduced to a single card, the BlackJack could serve both science and utility functions while consuming no more power, space, or dollars than a typical navigation instrument today.

FUTURE PROSPECTS

The question arises, how many sensors are enough? Much is expected scientifically from the emerging occultation array to consist of COSMIC (Taiwan, 6 satellites, 2005), EQUARS (Brazil-Japan, 2005), TerraSAR-X (Germany, 2006), ACE+ (European Space Agency, 2007?), and others to follow. For ocean reflections we've seen that a dozen could be of value. Perhaps the best hint of an upper limit on useful numbers comes from the recommendations of a national science panel convened by NASA in Easton, PA, in 1997. Their charter was to define the foreseeable scope of Earth remote sensing data needed in the next 10-15 years to address NASA's overall Earth science agenda. The Easton panel embraced GPS occultation and recommended that an operational constellation be deployed. A key requirement articulated for that system was to provide global atmospheric profiles with an average horizontal spacing of 50 km, twice per day, to initialize operational weather models. That translates to roughly 400,000 profiles per day. Achieving such numbers with a 60-satellite GNSS constellation will require 250-300 LEO sensors.

An array of eight or ten occultation sensors is, to be sure,

Plate 11

incomparably superior to none. It will represent a milestone as consequential as the early GPS geodetic networks. The marginal return for the next dozen will surely be less. But surveying the rich history of GNSS-based science, we have little doubt that the dividends will grow steadily with larger numbers, even into the hundreds. Global numerical weather prediction and snapshot 3D ionospheric imaging will be among the obvious beneficiaries. Whatever the value of the first ten sensors, it will be far surpassed by the value of 50.

Any effort we make now to catalogue the science to emerge from such an array is necessarily constrained by current concepts and paradigms. Sufficient changes in quantity, as Engels noted, at length become changes in quality. A global occultation array is a new breed of instrument for which have little experience or insight. Uncovering the riches within GNSS geodesy has taken two decades and continues still. That process has transformed our understanding of what is possible in measuring the Earth. A similar conceptual retooling will likely be required for Earth remote sensing with spaceborne GNSS. When all is said and done, the power and compass of this new tool will surely surpass what we can imagine now.

REFERENCES

Abshire, J. B. and S. Gardner (1985), Atmospheric refractivity corrections in satellite laser ranging, *IEEE Trans. Geosci. & Remote Sensing, 23*, 414-425.

Anthes, R. A, C. Rocken and Y.-H. Kuo (2000), Applications of COSMIC to meteorology and climate, in Lee et al. (2000), 115-156.

Ao, C. O., T. K. Meehan, G. A. Hajj, A. J. Mannucci, and G. Beyerle (2003), Lower-troposphere refractivity bias in GPS occultation retrievals, *J. Geophys. Res.*, 108(D18), 4577, doi:10.1029/2002JD003216.

Aoyama, Y., E. Ozawa and H. Tada (2003), Data assimilation experiment using temperature retrieved from CHAMP occultation data, Proc. Int. Workshop on GPS Meteorology, Tsukuba, Japan.

AVISO (2003), High-precision altimetry with satellites working together, http://www-aviso.cls.fr/html/alti/multi_sat_uk.html.

Beyerle, G. et al. (2003), The radio occultation experiment aboard CHAMP (Part II): Advanced retrieval techniques in atmospheric sounding and GPS reflectometry, Proc. Int. Workshop on GPS Meteorology, Tsukuba, Japan.

Beyerle, G. et al. (2002), GPS radio occultations with CHAMP: A radio holographic analysis of GPS signal propagation in the troposphere and surface reflections, *J. Geophys. Res.,* 107(D24), 4802, doi:10.1029/2001JD001402.

Beyerle, G; M. E. Gorbunov and C. O. Ao (2003a), Simulation studies of GPS radio occultation measurements, *Radio Sci.*, 39(5), 1084, doi:10.1029/2002RS002800.

Braun, J. and C. Rocken (2003), Slant water vapor in the United States southern Great Plains, Proc. Int. Workshop on GPS Meteorology, Tsukuba, Japan.

Cardellach, E., C. O. Ao., M. de la Torre Juarez and G. A. Hajj (2004), Carrier-phase delay altimetry with GPS-reflection/ occultation interferometry from low earth orbiters, submitted to *Geophys. Res. Lett.*

Cubasch et al. (2001), Projections of future climate change, In: *Climate Change 2001: The Scientific Basis*, Houghton, J. T. et al. (eds.), Cambridge Univ. Press, p. 555.

Davis, J. L., T. A. Herring, I. I. Shapiro, A. E. E. Rogers and G. Elgered (1985), Geodesy by radio interferometry: Effects of atmospheric modeling errors on estimates of baseline length, *Radio Sci., 20*, 1593-1607.

Elgered, G., B. Stoew, L. Gradinarsky and H. Bouma (2003), Analysis of atmospheric parameters derived from ground-based GPS observations, Proc. Int. Workshop on GPS Meteorology, Tsukuba, Japan.

Fjeldbo, G. (1964), Bistatic-radar methods for studying planetary ionospheres and surfaces, *Sci. Rpt. #2*, NsG-377, SU-SEL-64-025, Stanford Electronics Labs, Stanford, CA.

Fung, A. K, C. Zuffada and C.Y. Hsieh (2001), Incoherent bistatic scattering from the sea surface at L-band, *IEEE Trans. Geosci. and Rem. Sensing*, 39(5): 1006-1012.

Gorbunov, M. E. (2002), Canonical transform method for processing radio occultation data in the lower troposphere, *Radio Sci.* 37(5), doi:10.1029/2000RS002592.

Gorbunov M. E. (2001), Radioholographic methods for processing radio occultation data in multipath regions, *Danish Meteorological Inst. Scientific Report, 01-02*, Copenhagen.

Gorbunov, M. E., A. S. Gurvich, and L. Bengtsson (1996), Advanced algorithms of inversion of GPS/MET satellite data and their application to reconstruction of temperature and humidity, *Rep. 211*, Max Planck-Inst. Meteorol., Hamburg.

Gutman, S. I. et al. (2003), Rapid retrieval and assimilation of ground based GPS-Met observations at the NOAA Forecast Systems Laboratory: Impact on weather forecasts, Proc. Int. Workshop on GPS Meteorology, Tsukuba, Japan.

Ha, S.-Y., Y.-H. Kuo, G.-H. Lim (2003), Assimilation of GPS slant wet delay data and its impact on the short-range NWP, Proc. Int. Workshop on GPS Meteorology, Tsukuba, Japan.

Hajj, G. A. (1998), Reflections on GPS signal surface reflection, *JPL Memorandum*, 335-98-003.

Hajj, G. A. et al. (2004), CHAMP and SAC-C atmospheric occultation results and intercomparisons, *J. Geophys. Res.*, in press.

Hajj, G. A., E. R. Kursinski, L. J. Romans, W. I. Bertiger, S. S. Leroy (2002), A technical description of atmospheric sounding by GPS occultation, *J. Atmos. and Solar-Terrestrial Physics*, 64, 451-469.

Hajj, G. A. and C. Zuffada (2003), Theoretical description of a bistatic system for ocean altimetry using the GPS signal, *Radio Sci.*, 38(5), 1089, doi:10.1029/2002RS002787.

Hatanaka, Yuki (2003), Estimation of troposphere delay and accuracy of GEONET solutions, Proc. Int. Workshop on GPS Meteorology, Tsukuba, Japan.

Healy, S., A. Jupp and C. Marquardt (2003), A forecast impact trial with CHAMP radio occultation measurements, presented at EGS annual meeting, Nice, France, http://web.dmi.dk/pub/GRAS_SAF/presentations/egs-sh2-apr-2003.pdf.

Kliore, A. J., T. W. Hamilton, and D. L. Cain (1964), Determination of some physical properties of the atmosphere of Mars from changes in the Doppler signal of a spacecraft on an earth occultation trajectory, *Technical Report 32-674*, JPL.

Kuo,Y-H, T.-K. Wee and S. Sokolovskiy (2003), Analysis and assimilation of radio occultation data, Proc. Int. Workshop on GPS Meteorology, Tsukuba, Japan.

Kursinski E. R., Healy S. B., Romans L. J. (2000), Initial results of combining GPS occultations with ECMWF global analyses within a 1DVar framework, *Earth Planets and Space, 52* (11): 885-892.

Kursinski, E. R. and G. A. Hajj (2001), A comparison of water vapor derived from GPS occultations and global weather analyses, *J. Geophys. Res.*, 106(D1): 1113-1138.

Kursinski, E. R., G. A. Hajj, K. R. Hardy, J. T. Schofield, and R. Linfield (1997), Observing Earth's atmosphere with radio occultation measurements, *J. Geophys. Res.*, 102(D19): 23429-23465.

Lee, L., C. Rocken and E. Kursinski, eds. (2000), *Applications of Constellation Observing System for Meteorology, Ionosphere & Climate*, Springer-Verlag, ISBN 962-430-135-2.

Leroy, S. S. (1997), Measurement of geopotential heights by GPS radio occultation, *J. Geophys. Res.*, 102, 6971-6986.

Lichten, S. M. and W. I. Bertiger (1989), Demonstration of sub-meter GPS orbit determination and 1.5 parts in 10^8 three-dimensional baseline accuracy, *Bull. Geod., 63*, 167-189.

Lichten, S. M. and J. S. Border (1987), Strategies for high-precision Global Positioning System orbit determination, *J. Geophys. Res., 92*, 12751-12762.

Lowe, S. T. et al. (2002), First spaceborne observation of an Earth-reflected GPS signal, *Radio Sci.*, 37(1), article 1007.

Mann, M. et al. (2003), On past temperatures and anomalous late-20th century warmth, *EOS, Trans. AGU* 84(27): 256-257.

Martin-Neira, M. (1993), A passive reflectometry and interferometry system (PARIS): application to ocean altimetry, *ESA Journal*, 17, 331-355.

Melbourne, W.G. et al. (1994), *The Application of Spaceborne GPS to Atmospheric Limb Sounding and Global Change Monitoring*, JPL Publication 94-18.

NASA (2002), Cooperative Agreement Notice CAN-02-OES-01, Earth Science Research, Education and Applications Solutions Network (REASoN).

Palmer, P. I., J. J. Barnet, J. R. Eyre, S. B. Healy (2000), A non-linear optimal, estimation inverse method for radio occultation measurements of temperature, humidity, and surface pressure, *J. Geophys. Res.—Atmos.,* 105(D13): 17513-17526.

Picardi, G., R. Seu, S. G. Sorge and M. Martin-Neira (1998), Bistatic model of ocean scattering", *IEEE Trans. Antennas and Propagation*, 46(10): 1531-1541.

Raney, R.K. (2001a), Bistatic WITTEX Altimetry, *SRO-01-05*, Johns Hopkins University, Applied Physics Laboratory.

Raney, R. K. and D. L. Porter (2001b), WITTEX: An innovative multi-satellite radar altimeter constellation: A summary state-

ment for the high-resolution ocean topography science WG, http://www.deos.tudelft.nl/gamble/docs/wittex.pdf.

Ridal, M. and N. Gustafsson (2003), Assimilation of ground-based GPS data within the European COST-716 action, Proc. Int. Workshop on GPS Meteorology, Tsukuba, Japan.

Rocken, C. et al. (1997), Verification of GPS/MET data in the neutral atmosphere, *J. Geophys. Res.*, 102, 29,849-29,866.

Rodriguez, E. and B.D. Pollard (2002), The measurement capabilities of wide-swath ocean altimeters, GAMBLE web site: http://www.deos.tudelft.nl/gamble/documents.shtml

Shoji, Y. et al. (2003), Improvement of GPS analysis of slant path delay by stacking one-way postfit phase residuals, Proc. Int. Workshop on GPS Meteorology, Tsukuba, Japan.

Sokolovskiy, S. (2002), Fundamentals of open-loop tracking of radio occultation signals in the lower troposphere, Proc. OPAC-1 International Workshop, Graz, Austria.

Sokolovskiy, S. V. (2001a), Modeling and inverting radio occultation signals in the moist troposphere, *Radio Sci.,* 36(3): 441-458,

Sokolovskiy, S. (2001b), Tracking tropospheric radio occultation signals from low Earth orbit, *Radio Sci.*, 36(3), doi:10.1029/1999RS002305.

Sokolovskiy, S (2003), Effect of superrefraction on inversions of radio occultation signals in the lower troposphere, *Radio Sci.,* 38(3), 1058, doi:10.1029/2002RS002728.

Stammer D., C. Wunsch and R. M. Ponte (2000), De-aliasing of global high frequency barotropic motions in altimeter observations *Geophys. Res. Lett.,* 27 (8): 1175-1178.

Treuhaft, R. N., Y. Chao, S. T. Lowe, L. E. Young, C. Zuffada and E. Cardellach (2003), Monitoring coastal eddy evolution with GPS altimetry, Proc. Int. Workshop on GPS Meteorology, Tsukuba, Japan.

Vinnikov and Grody (2003), Global warming trend of mean tropospheric temperature observed by satellites, *Science 302* (5643): 269-272.

Yunck, T. P., C.-H. Liu and R. Ware (2000), A history of GPS sounding, in Lee et al. (2000), pp. 1-20.

Yunck, T. P., G. F. Lindal and C.-H. Liu (1988), The role of GPS in precise Earth observation, *Proc. IEEE Position Loc. and Nav. Symp. (PLANS 88)*, Orlando, FL, 251-258.

Zavorotny, V.U. and A. G. Voronovich (2000), Scattering of GPS signals from the ocean with wind remote sensing application, *IEEE Trans Geosci. and Rem. Sensing*, 8(2): 951-964.

Zou, X., H. Liu and H. Shao (2003), Further investigations on the assimilation of GPS occultation measurements, Proc. Int. Workshop on GPS Meteorology, Tsukuba, Japan.

Thomas P. Yunck
M/S 126-347
Jet Propulsion Laboratory
4800 Oak Grove Drive
Pasadena, CA 91109

George A. Hajj
M/S 238-600

Jet Propulsion Laboratory
4800 Oak Grove Drive
Pasadena, CA 91109

FIGURE CAPTIONS

Plate 1. GEONET PW maps over a 3-day period in September 2001.

Plate 2. Impact of GPS data on 12-hr predictions of relative humidity in the US at 4 pressure levels over 3 years. Positive value indicates improvement (from *Gutman et al*. 2003).

Plate 3. Observing geometry for atmospheric limb sounding by GPS radio occultation.

Plate 4. Distribution of soundings in 1 day with 1 receiver and 24 GPS satellites.

Plate 5. Projected change in average global surface temperatures over the next century according to several climate models (from *Cubasch et al*., 2001).

Plate 6. GPS/MET profile compared against a radiosonde and ECMWF analysis. Discrepancies are consistent with the expected accuracies of the comparison standards (from *Kursinski et al*., 2000).

Plate 7. Average of several hundred GPS/MET profiles differenced against ECMWF analyses. The mean agreement (dark line) is at the level of ~1 K (from *Hajj et al*., 2002).

Plate 8. Coincident profile pair from CHAMP and SAC-C plotted against NCEP and ECMWF analyses at each profile location (left); and the average differences of several dozen coincident pairs at five different maximum separations (right) (from *Hajj et al*., 2003.)

Plate 9. Spectrogram of an occultation from CHAMP after known Doppler shifts have been removed (bright vertical feature). Also visible is a faint surface reflection moving from the far left (about halfway up) to the lower right. Direct modeling would enhance the reflection (from *Hajj et al*., 2003).

Plate 10. The BlackJack GPS occultation receiver now flying on CHAMP and SAC-C. Inset shows a commercial 12-channel GPS receiver found in some cell phones and watches.

Plate 11. Concept for future occultation instrument exploiting modern LSI technology.

Figure 1. Summary of 4,043 CHAMP profiles made with geometric optics (blue) and canonical transform retrieval techniques, differenced with ECMWF analyses. Standard deviations (left) and mean offsets (center) are similar to those of GPS/MET (from *Beyerle et al.*, 2003).

Figure 2. Ocean coverage achieved in one day from one receiver in LEO collecting reflections from 24 GPS satellites (from *Hajj and Zuffada*, 2003)

Figure 3. Plots of the ideal GPS auto-correlation function with no multipath (left) and of a reflection from the ocean surface cross-correlated with a model signal at many different lags, for four different surface wind speeds.

Figure 4. Estimated net reflected range errors for a 4-sec averaged measurement as a function of the angle off nadir, for 5 different receiver antenna gains.

Figure 5. Average number of visible reflections per degree of off-nadir angle (red) and cumulative from nadir outward, as a function of the off-nadir viewing angle (from *Hajj and Zuffada*, 2003).

Figure 6. The nominal wave height at which the reflected carrier phase loses coherence, based on the Rayleigh criterion (from *Hajj*, 1998).

Figure 7. The differing geometries of reflections acquired near nadir and at the horizon.

Figure 8. Occultations acquired by CHAMP between 14 May and 10 June of 2001 (dots) and accompanying reflections (circles). Circle size indicates relative strength (from *Beyerle et al.*, 2002).

GNSS ATMOSPHERIC SOUNDING AND ALTIMETRY

GNSS ATMOSPHERIC SOUNDING AND ALTIMETRY

GNSS ATMOSPHERIC SOUNDING AND ALTIMETRY

GNSS ATMOSPHERIC SOUNDING AND ALTIMETRY

GNSS ATMOSPHERIC SOUNDING AND ALTIMETRY

GNSS ATMOSPHERIC SOUNDING AND ALTIMETRY

GNSS ATMOSPHERIC SOUNDING AND ALTIMETRY

GNSS ATMOSPHERIC SOUNDING AND ALTIMETRY

GNSS ATMOSPHERIC SOUNDING AND ALTIMETRY

GNSS ATMOSPHERIC SOUNDING AND ALTIMETRY

GNSS ATMOSPHERIC SOUNDING AND ALTIMETRY

GNSS ATMOSPHERIC SOUNDING AND ALTIMETRY

GNSS ATMOSPHERIC SOUNDING AND ALTIMETRY

GNSS ATMOSPHERIC SOUNDING AND ALTIMETRY

GNSS ATMOSPHERIC SOUNDING AND ALTIMETRY

GNSS ATMOSPHERIC SOUNDING AND ALTIMETRY

GNSS ATMOSPHERIC SOUNDING AND ALTIMETRY

YUNCK AND HAJJ

YUNCK AND HAJJ

YUNCK AND HAJJ

YUNCK AND HAJJ

YUNCK AND HAJJ

YUNCK AND HAJJ

YUNCK AND HAJJ

YUNCK AND HAJJ

YUNCK AND HAJJ

YUNCK AND HAJJ

YUNCK AND HAJJ

YUNCK AND HAJJ

YUNCK AND HAJJ

YUNCK AND HAJJ

YUNCK AND HAJJ

YUNCK AND HAJJ

YUNCK AND HAJJ

Plate 1

Plate 2

LEO Receiver   Signal Raypath   To GPS →

Plate 3

Plate 4

Plate 5

29

Santa Cruz Islands
5 April 1995

Occultation Retrieval, 7.9S, 167.5E
Radiosonde, 12hr UT, 6.0S, 170.4E
ECMWF Global Model, 12hr, UT

Plate 6

30
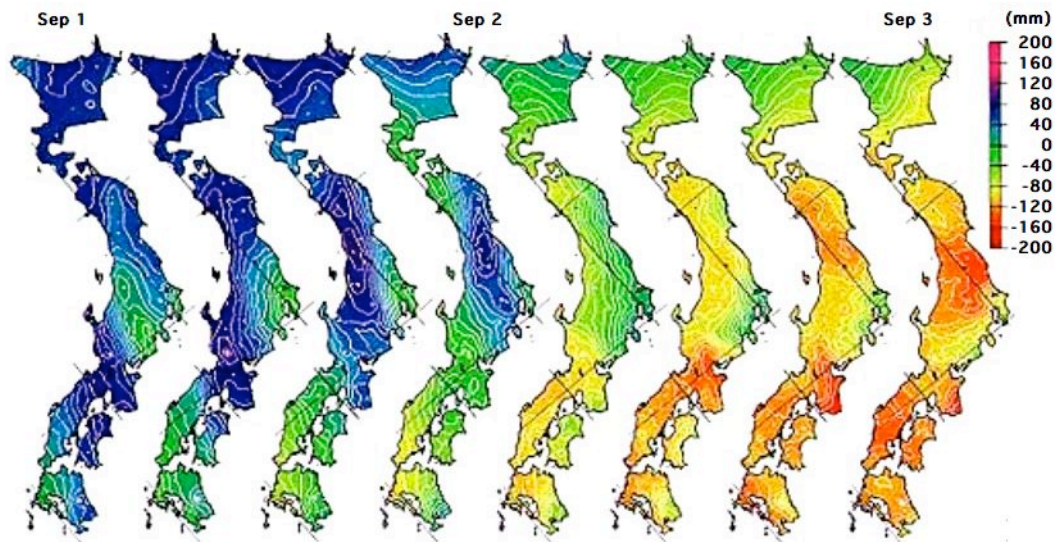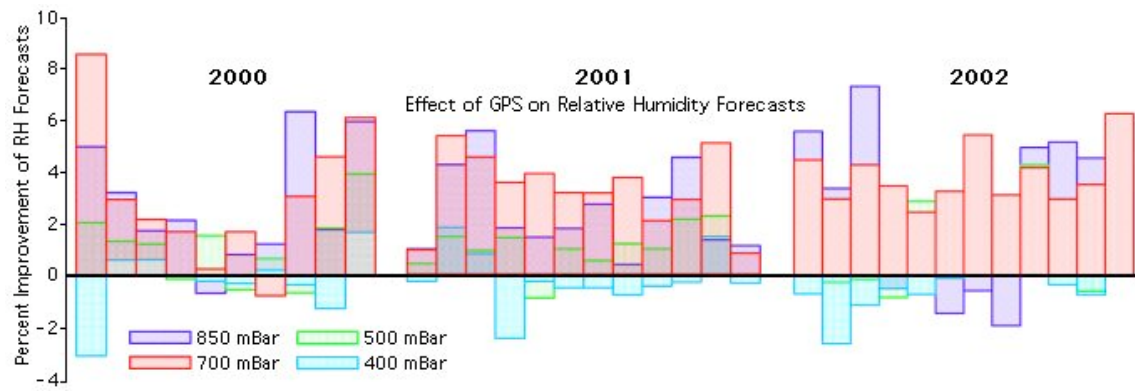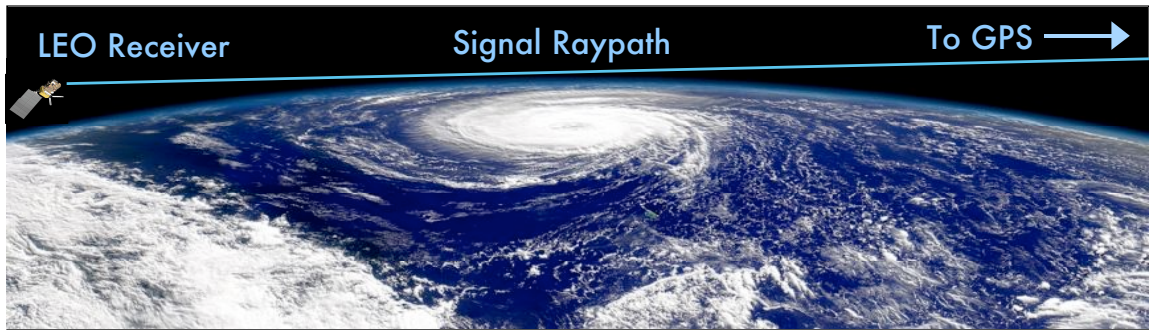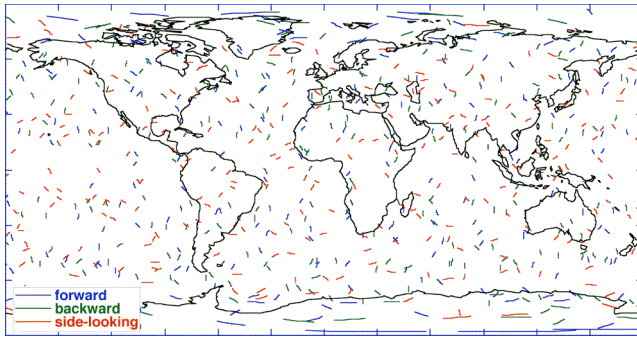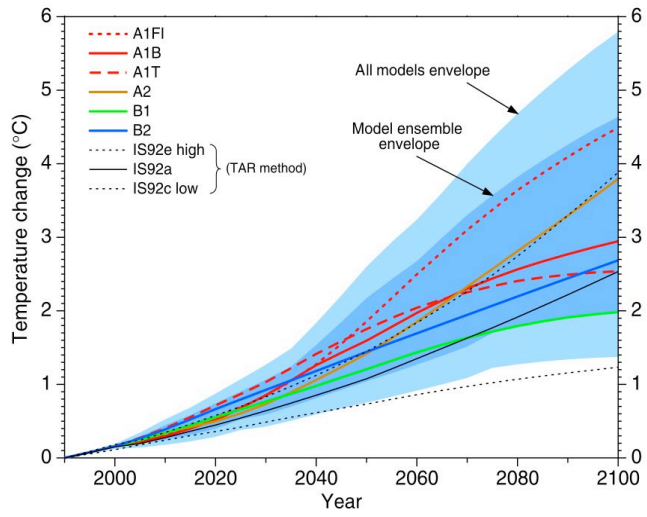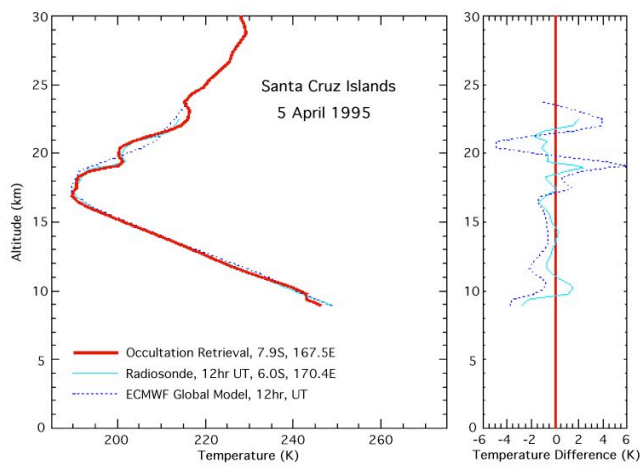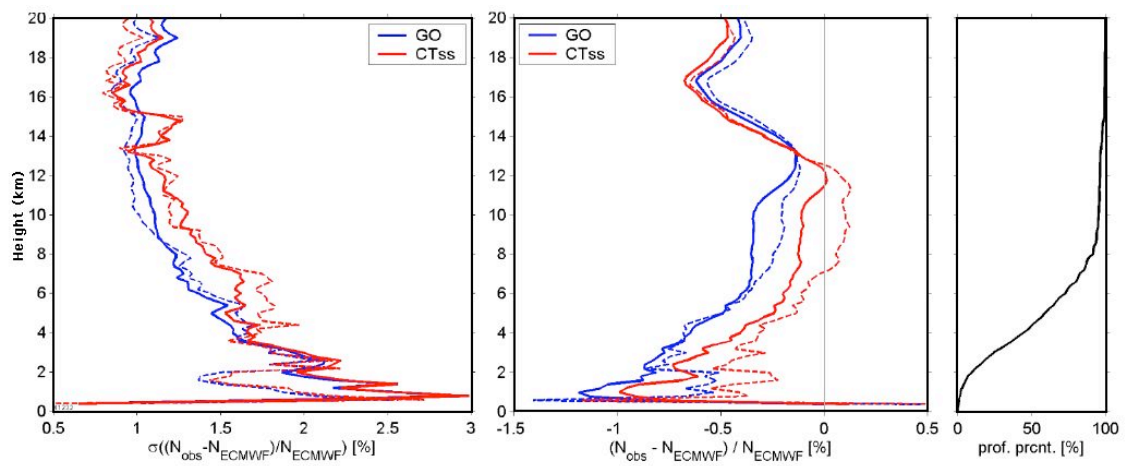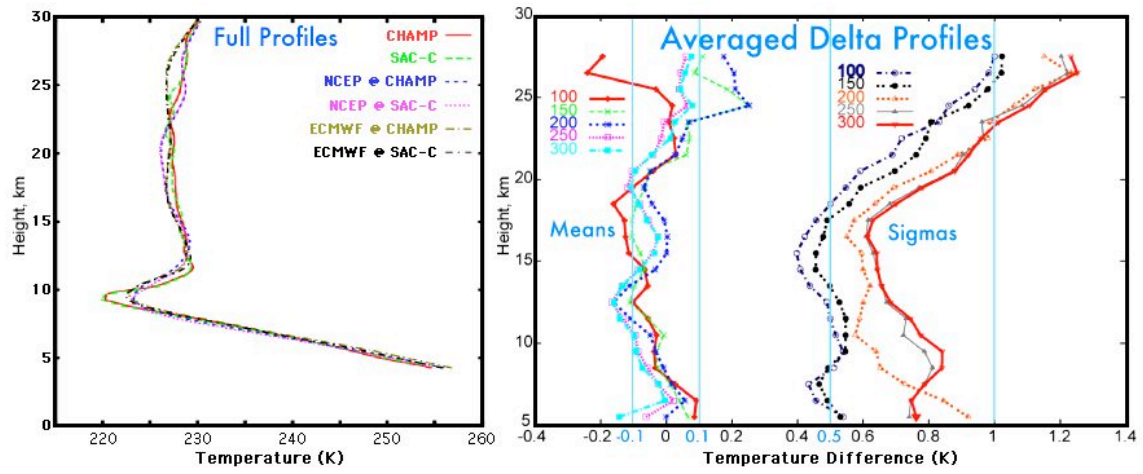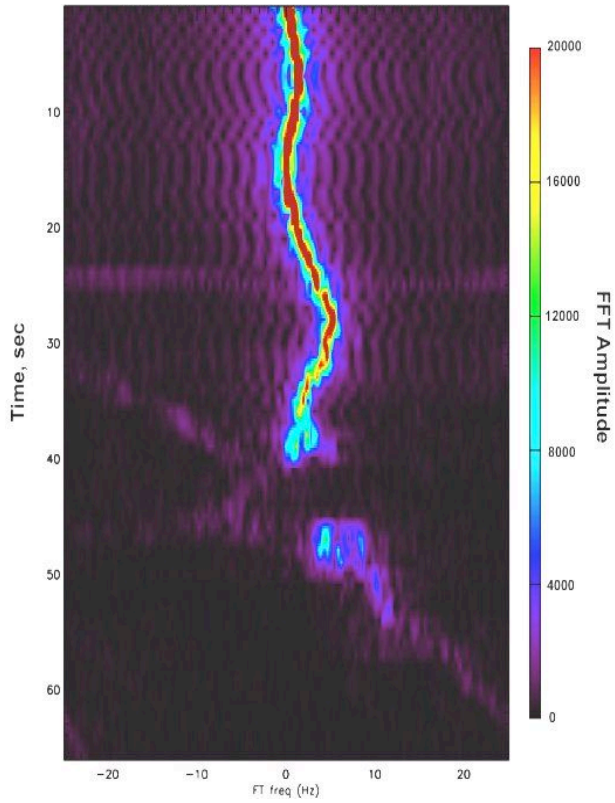
Plate 7
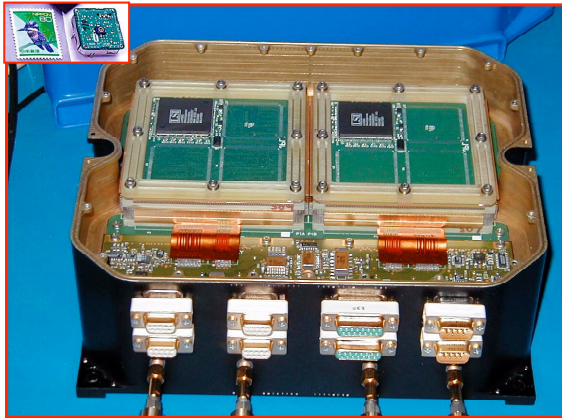
Plate 8

Plate 9

Plate 10
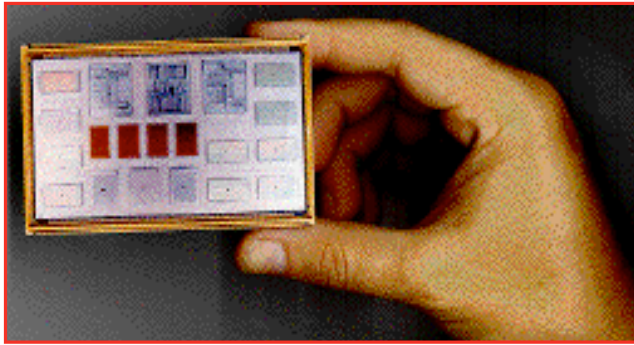
Plate 11
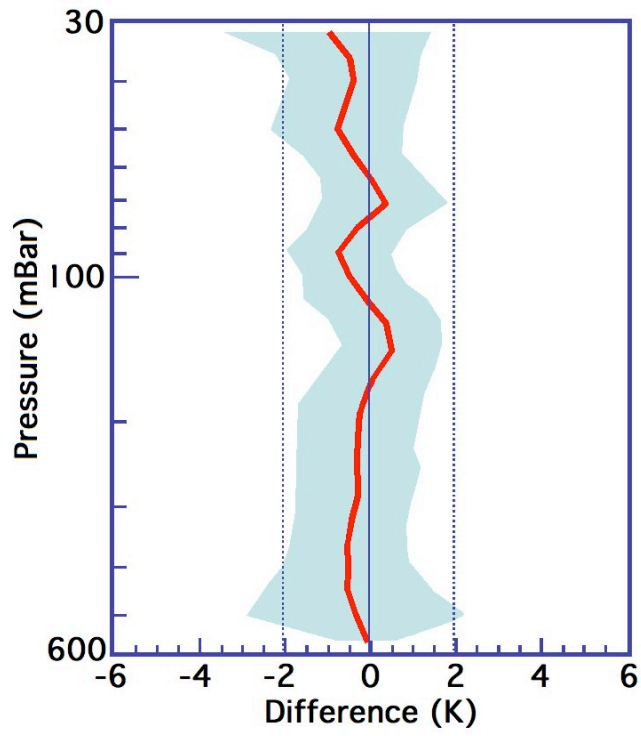
Fig. 1
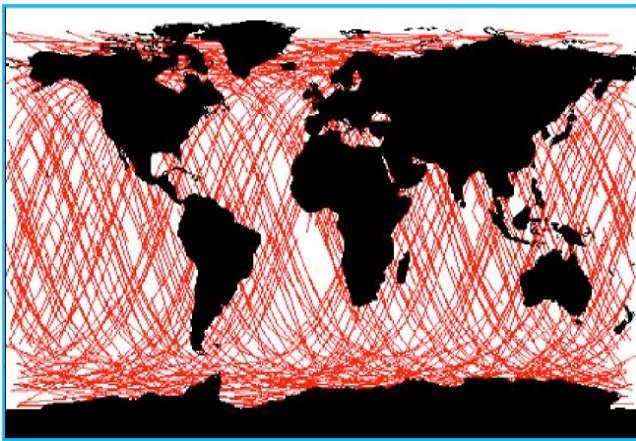
Fig. 2

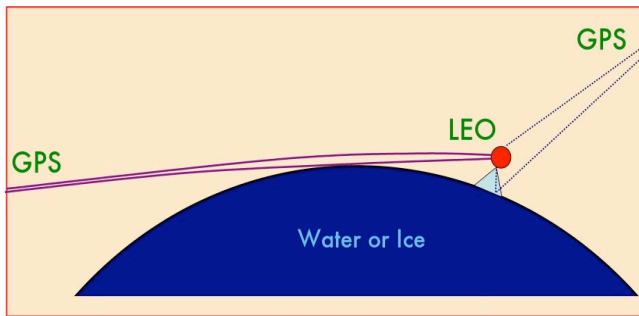**Fig. 3**
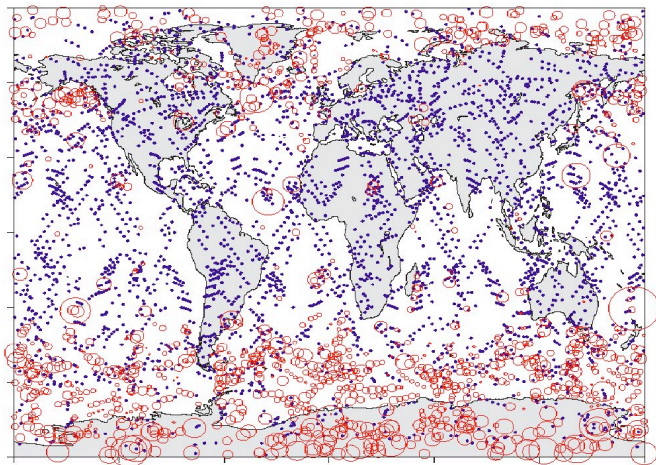
Fig. 4

Fig. 5

40
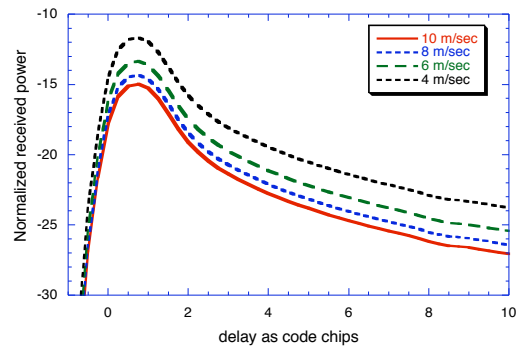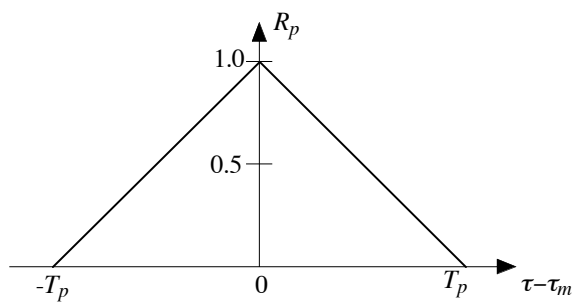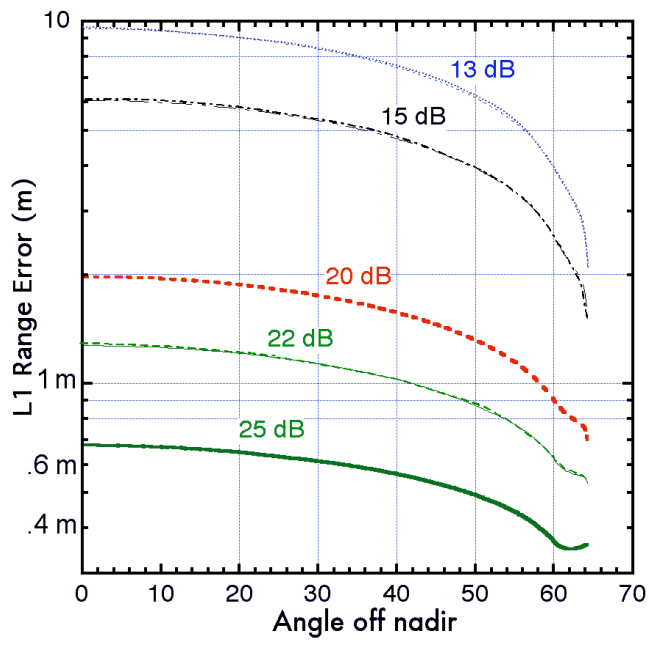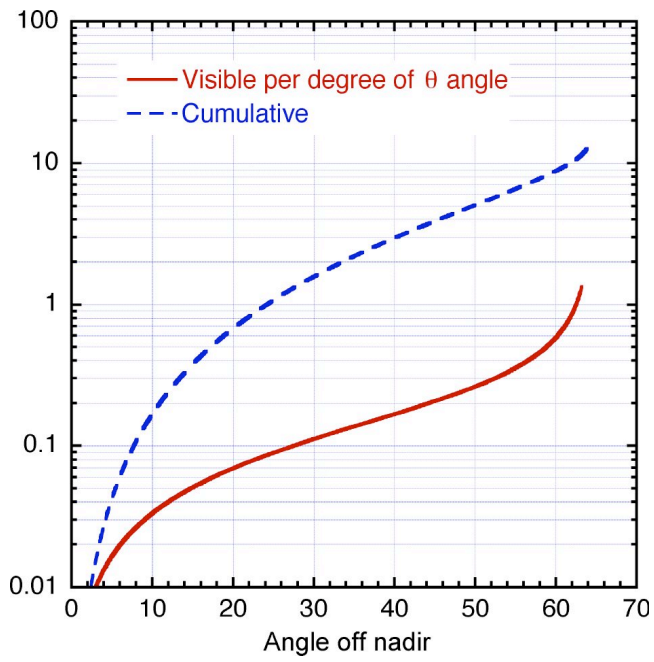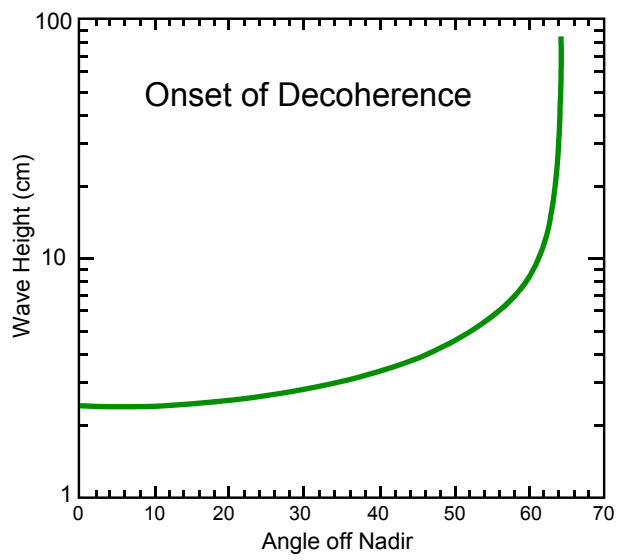
Fig. 6

Fig. 7

Fig. 8

Table 1. Seven Attractions of GNSS Occultation

- Offers order-of-magnitude improvement in accuracy and long-term stability of atmospheric temperature profiles.
- Operates undiminished in all weather, day or night.
- Offers near-uniform global coverage from the upper stratosphere to the surface.
- Provides vertical resolution to better than 100 m throughout the troposphere.
- Yields absolute heights of measured quantities to better than 10 m, permitting derivation of global pressure contours and non-equatorial geostrophic wind fields.
- Exploits different physical principles from other atmospheric sensors, remote or in situ, presenting an independent comparison and calibration standard.
- Requires only a palm-sized module costing <1 % of the tens to hundreds of M$ of many of today's passive sensors.